Nuclear Engineering and Technology 53 (2021) 2839–2846

Contents lists available at ScienceDirect

Nuclear Engineering and Technology

journal homepage: www.elsevier.com/locate/net

Original Article

A preliminary study on material effects of critical heat flux for downward-facing flow boiling

Kai Wang [a], Chun-Yen Li [a, *], Kotaro Uesugi [a], Nejdet Erkan [a], Koji Okamoto [b]

[a] Department of Nuclear Engineering and Management, School of Engineering, The University of Tokyo, 7-3-1 Hongo, Bunkyo-ku, Tokyo, 113-8654, Japan
[b] Nuclear Professional School, School of Engineering, The University of Tokyo, 2-22 Shirakata, Tokai-mura, Ibaraki, 319-1188, Japan

ARTICLE INFO

Article history:
Received 3 May 2020
Received in revised form
27 February 2021
Accepted 26 March 2021
Available online 1 April 2021

Keywords:
Critical heat flux
Flow boiling
Bubble behavior
Wettability
Surface roughness

ABSTRACT

In this study, experiments of downward-facing flow boiling were conducted to investigate material effects on CHF. Experiments were conducted using aluminum, copper, and carbon steel. It was found that different materials had different CHFs. Aluminum has the biggest CHF while copper has the lowest CHF for each mass flux. After experiment, surface wettability increased and surface became rougher, which was probably due to the oxidation process during nucleate boiling. The CHF difference is likely to be related to the surface wettability, roughness and thermal effusivity, which influences the bubble behavior and in turn affects CHF. Further studies are needed to determine which factor is dominant.

1. Introduction

Over the past decades, there is a drastic growing demand for heat dissipation in various fields such as heat exchangers, reactors, or electronics [1,2]. Due to its nature of high heat transfer efficiency, nucleate boiling has been widely studied. Compared to a single-phase heat transfer method, nucleate boiling with phase change has a greater heat transfer coefficient. However, there is a boiling crisis known as critical heat flux (CHF), which strongly restricts the utilization of the nucleate boiling. If further heat flux over CHF was supplied, the heater surface underwent a surge in temperature and was seriously damaged, which could be disastrous [3]. For example, in new reactors such as AP1000, a mitigation method, In-vessel retention external reactor vessel cooling (IVR-EVRC), was introduced to remove the decay heat generated by phase change if severe accidents occurred [4]. The integrity of the reactor pressure vessel (RPV) can be guaranteed if a boiling crisis does not occur. However, if heat flux was greater than CHF value, RPV might fail, which strongly endangered the safety of the lower plenum. Although there was no census on the mechanism of CHF, there has been many studies on enhancing CHF.

The CHF variation was attributed to the heater surface properties such as wettability, wall size, thickness, thermal properties, and surface roughness. For example, Lee et al. [5] oxidized zircaloy test pieces under three different temperatures. They found an 40% enhancement of CHF for oxidized pieces compared to non-oxidized ones. The CHF enhancement was attributed to the increased wettability of the surface, which was later compared to a correlation proposed by Kandlikar [6]. This correlation tried to demonstrate a relationship between CHF and single bubble parent contact angle. The good agreement between experimental results and the correlation indicated the feasibility of explaining CHF enhancement by wettability change. Wang et al. [7,8] studied the gradual increase of CHF by water oxidation for pool boiling and flow boiling, separately. They stated that the enhancement of CHF might result from combined effects of contact angle and nucleation site density (NSD) change. For the surface roughness effect, O'Hanley et al. [9] studied the effect of roughness by fabricating different particle-coated surfaces. The results indicated that CHF was independent of roughness. However, Kim et al. [10] changed the roughness of copper and observed an enhancement of CHF with the increase of roughness. A correlation related to the surface roughness was also proposed to explain the roughness effect.

Another important property which influenced heat transfer coefficient and CHF was heater material. Braun [11] conducted pool boiling experiments using tubes made of copper, brass and steel.

* Corresponding author. 7-3-1 Hongo, Bunkyo-ku, Tokyo, 113-8654, Japan.
E-mail address: lchihar@gmail.com (C.-Y. Li).

https://doi.org/10.1016/j.net.2021.03.024

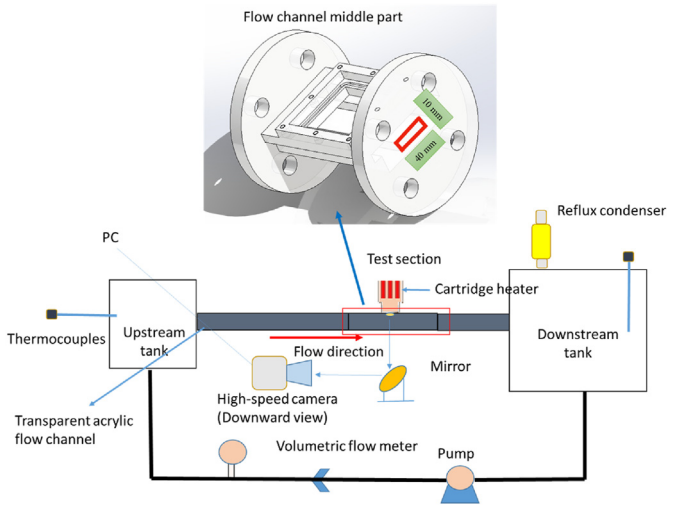

Fig. 1. Schematic overview of the experimental apparatus.

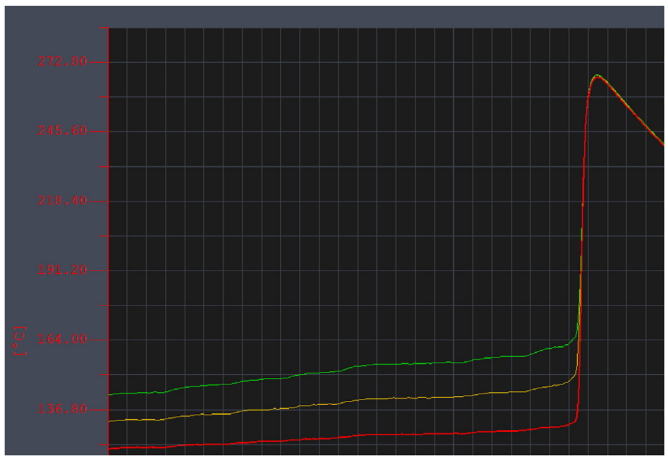

Fig. 3. Example of a recorded temperature profile for aluminum.

Table 1
Experimental uncertainties.

Parameter	Range	Uncertainty
Temperature	243.5–700 K	0.75%
Length	0–6 mm	3.3%
Thermal conductivity	N/A	0.76%
Mass flux	0–40 L/min	0.5%
Inlet temperature	Around 100 °C	1%
Heat flux	0–2.0 MW/m^2	3.5%
Superheating for Cu/Al	1–30 K	3.7%
CS plate	1.0 mm	1%
Thermal insulance of silver paste	N/A	3.6%
Superheating for CS	1–30 K	5.3%

Although the roughness of different materials was kept similar, images of the heater surface showed significant different NSD conditions. Zhou and Bier [12] studied the effect of copper layer thickness coated on steel tubes. It was found that more bubbles were generated on thicker layer surface. The thicker layer surface had a bigger heat transfer coefficient. Magrini and Nannei [13] studied the wall thickness and thermal conductivity effect using rods coated with different materials such as copper, silver, zinc and nickel. Experimental results showed that both wall thickness and thermal conductivity influenced NSD and heat transfer. Grigoriev et al. [14] investigated effects of heater materials by pool boiling experiments. They found that different CHF could be explained by the thermal effusivity. Westwater et al. [15] tried to explain the thermal effusivity effect by its assistance in heat dissipation process. Mei et al. [16] conducted pool boiling experiments on copper, SA508 and stainless steel and found that different CHFs could be well explained by different thermal effusivity of materials. Bombardieri et al. [17] investigated material effects in pool boiling experiments using liquid nitrogen. Different materials had different CHFs, but it was difficult to explain by the thermo-physical properties. Lee and Chang [18] used a ribbon test heater made of SA508 and SS304. It was found that CHF increased with boiling time with a peak at 50 min. The CHF of SA508 was higher than that of SS304. Park et al. [19] conducted a flow boiling experiment to study SA508 and stainless steel CHF with additive solutions. It was found that due to the oxidation, SA508 has a higher CHF than that of stainless steel. Kam et al. [20] carried out a pool boiling experiment under different pressures using carbon steel and stainless steel. It was found that under all different conditions carbon steel showed higher CHF than stainless steel. They pointed out that surface parameters like thermal properties could be considered to explain the CHF difference. Later, they developed a dry-spot theory to explain CHF under different conditions [21]. Although many studies investigated effects of materials, there was no census on the mechanism. By using different material, many variables such as thermal conductivity, roughness and microstructure changed at the

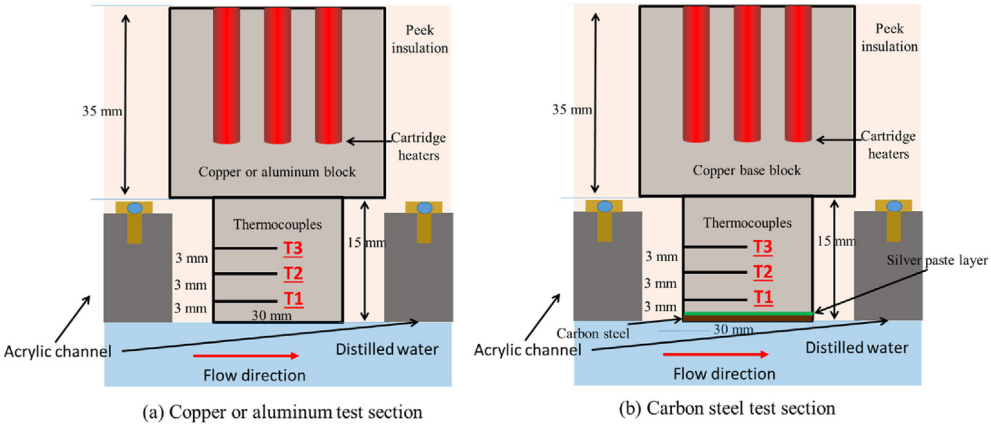

Fig. 2. Test section schematic diagram.

Table 2
Experimental conditions.

Parameters	Value
Pressure	Atmosphere
Boiling area	30 × 30 mm in square
Subcooling	Saturated
Mass flux (kg/(m^2 s))	160, 320
Materials	Copper, carbon steel, and aluminum

same time, making it very difficult to tell which factor affected boiling most.

Due to the low thermal conductivity of carbon steel, many studies used copper as the base material to study the effect of contact angle [22], roughness [10], copper microporous surface layers [23], honeycomb structure [24] and so on. However, research also showed that different materials had exhibited different boiling behavior and CHFs greatly. Experimental results of the copper may not be easily transferred to other materials. In this study, a preliminary study on material effects of CHF for downward-facing flow boiling is presented. The research of material effect for downward-facing flow boiling is rather scare. The necessity of studying downward-facing flow boiling originates from the different mechanism behind downward-facing boiling from upward-facing or vertical boiling. In downward-facing boiling, the buoyancy force was inverse with the normal of the heater surface. Bubbles were prone to coalesce and accumulate on the surface, which led to an earlier boiling crisis. In the case of EVRC in nuclear reactors, the liquid flows through the lower plenum. Therefore, experiments of material effects on CHF for downward-facing flow boiling were conducted.

2. Experimental setup and procedure

2.1. Experimental setups

Fig. 1 shows a schematic view of the test facility. The flow channel was made of acrylic for visualization purpose. The middle part of the flow channel has a 40 mm in width and 10 mm in height. A test section shown in Fig. 2 was inserted to the middle of the channel by screws. A high-speed camera typed FASTCAM SA4 was used to record images from the downward direction, which operated at a resolution of 1024 × 1024, 1000 fps. A magnetic pump with a maximum flow rate of 40 L/min was connected to the loop. A flow rate meter with a flow range of 2.8–45 L/min was utilized to measure the flow rate. There are two tanks denoted as upstream tank and downstream tank to store distilled water. Two thermocouples were inserted to the two tanks and connected to a data logger. The experiment was conducted under atmospheric pressure. To make sure water was maintained at saturation temperature, the temperature of the two tanks was monitored during the experiment. In the downstream tank, a reflux condenser was installed to cool down the steam. The temperatures of the two tanks were kept at 99.5 ± 0.5 °C by adjusting the heater.

Fig. 2 shows test sections for the experiment. There are three kinds of test sections. For copper and aluminum, they share the same configuration as shown in Fig. 2 (a). The copper/aluminum block was heated by nine cartridge heaters inserted to the top of the block. Polyether ether ketone (PEEK) was used to cover the block for insulation purpose. The block has a 40 × 40 mm rectangular on top part and a 30 × 30 mm rectangular on down part. Three thermocouples were inserted into the holes distributed every 3 mm. The temperatures of three points can be used to calculate the surface temperature as well as the heat flux by a one-dimensional Fourier law. Moreover, a three-temperature point least-square

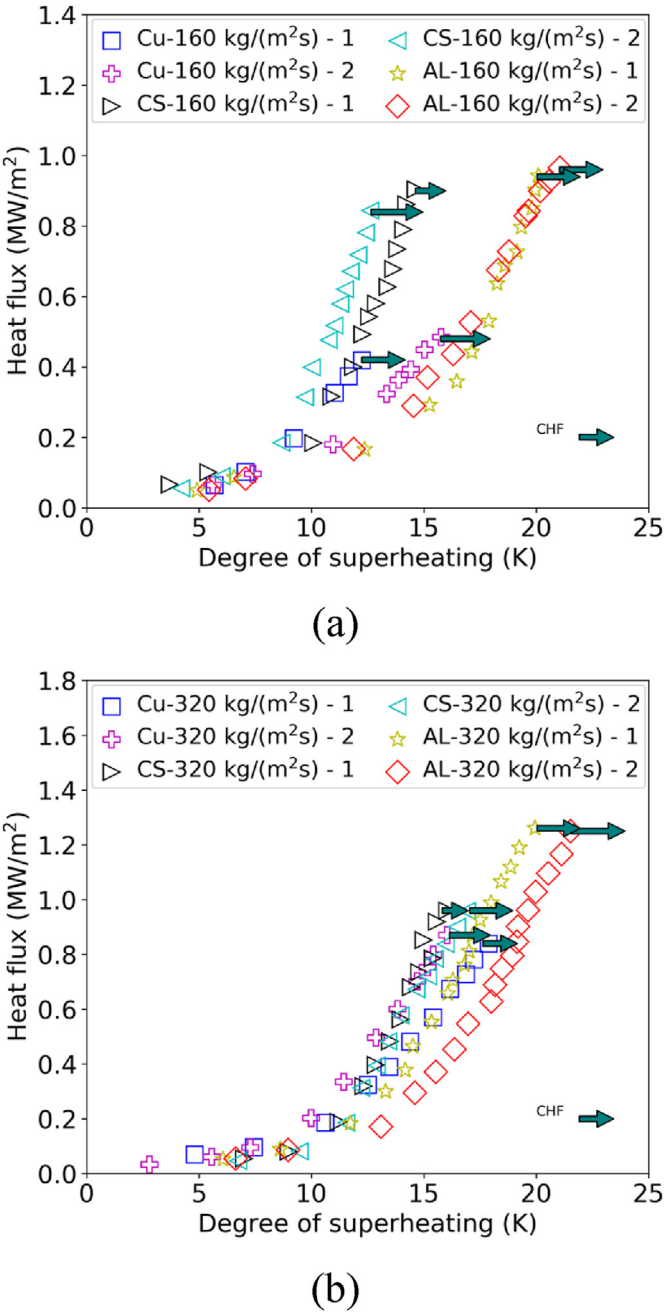

Fig. 4. Boiling curves for different materials under different mass fluxes. Experiments conducted at mass flux of (a) 160 kg/(m^2 s), (b) 320 kg/(m^2 s).

fitting method was used to calculate the temperature gradient.

$$T_{wall} = T_1 - q'' \frac{\delta_{cu/al}}{k_{cu/al}} \tag{1}$$

$$q'' = k_{cu/al} \frac{dT}{dx} \tag{2}$$

$$\frac{dT}{dx} = \frac{3^* \sum x_i T_i - \sum x_i \sum T_i}{3^* \sum x_i^2 - (\sum x_i)^2} \tag{3}$$

where $\delta_{cu/al}$ is the length of the thermocouple hole to the surface;

$k_{cu/al}$ is the thermal conductivity of the copper or aluminum, and q'' is the heat flux rate, and x denotes the distance between the thermocouples. x_i is the distance from the down face to the thermocouple, and i = 1, 2, 3. T_i is the temperature of the corresponding thermocouple.

For carbon steel, we used a different test section shown in Fig. 2 (b). A carbon steel plate with a thickness of 1.0 mm was attached to the copper base surface by silver solder method. This is because carbon steel has a relatively low thermal conductivity ($50\ W/(m\cdot K)$) compared to copper and aluminum ($400\ W/(m\cdot K)$ and $237\ W/(m\cdot K)$, respectively).

Golobič and Bergles [25] pointed out that if the thickness of the plate exceeded a certain value, the thermal effusivity no longer had an effect on CHF. For carbon steel, the thickness was approximately 0.36 mm. In our experiment, the thickness of the carbon steel was 1 mm, so it was thick enough to reduce the thermal effusivity effect. Then we attached a thermocouple to the bottom of the surface and changed the heat flux to measure the thermal insulance of the silver paste. As the thickness of the silver paste was also difficult to measure, we did not calculate the thermal conductivity of the silver paste. Instead, we measured the thermal insulance of the silver paste, R_{solder} was measured to be around $6.7*10^{-5}\ (m^2\cdot K/W)$. Then the heat flux can be calculated by Eqs. (2) and (3). The surface temperature can be calculated by

$$T_{wall} = T_1 - q''\left(\frac{\delta_{cs}}{k_{cs}} + \frac{\delta_{cu}}{k_{cu}} + R_{solder}\right) \tag{4}$$

where δ_{cu} and δ_{solder} are the length of the copper and carbon steel, respectively. k_{cu}, and k_{cs} are the thermal conductivity of the copper, carbon steel, respectively. R_{solder} is the thermal insulance of the solder.

2.2. Experimental procedures

Before the experiment, each surface was polished by sandpapers P1200. Then acetone was used to clean the surface after polishing. Then the block was installed to the test channel. Distilled water was supplied to the test loop and heated up to saturation temperature and degassed for about 0.5 h. Then, the experiment started. Heat flux was supplied to the block by cartridge heaters. The voltage was increased every 10 V at the beginning, then every 5 V when it came close to a boiling crisis. Heat flux was increased about 0.05 MW/m^2 during the experiment, which corresponded to an increase of about 0.4 °C for temperature gradient between two thermocouples for copper (about 0.6 °C for aluminum). At every step, if the temperature could hold for several minutes, then it was considered as a steady state. We recorded images by a high-speed camera. This step was repeated until a sudden surge in temperature profile occurred (always more than 50 °C), then it was considered that CHF happened. Meanwhile, a large vapor film formed and covered the surface. We stopped the experiment by shutting down all heaters and waited the facility to cool down. Fig. 3 shows an example of the recorded temperature profile of aluminum, which was later used to calculate the degree of superheating and heat flux.

2.3. Uncertainty analysis

We used Moffat [26] method to estimate the uncertainty of CHF and superheating.

$$\frac{\delta R}{R} = \sqrt{\left(\frac{\delta u_1}{u_1}\right)^2 + \left(\frac{\delta u_2}{u_2}\right)^2 + \cdots + \left(\frac{\delta u_n}{u_n}\right)^2} \tag{5}$$

Uncertainty of heat flux was calculated as

$$\frac{\delta q''}{q''} = \sqrt{\left(\frac{\delta k_{cu}}{k_{cu}}\right)^2 + \left(\frac{\delta x}{x}\right)^2 + \left(\frac{\delta T_1}{T_1}\right)^2 + \left(\frac{\delta T_3}{T_3}\right)^2} \tag{6}$$

Uncertainties of the aluminum/copper and carbon steel are calculated, respectively

$$\frac{\delta T_{sup-AL/Cu}}{T_{sup-AL/Cu}} = \sqrt{\left(\frac{\delta T_{in}}{T_{in}}\right)^2 + \left(\frac{\delta k_{cu}}{k_{cu}}\right)^2 + \left(\frac{\delta x}{x}\right)^2 + \left(\frac{\delta T_1}{T_1}\right)^2 + \left(\frac{\delta T_3}{T_3}\right)^2} \tag{7}$$

$$\frac{\delta T_{sup-CS}}{T_{sup-CS}} = \sqrt{\left(\frac{\delta T_{in}}{T_{in}}\right)^2 + \left(\frac{\delta k_{cu}}{k_{cu}}\right)^2 + \left(\frac{\delta x_{cu}}{x_{cu}}\right)^2 + \left(\frac{\delta T_1}{T_1}\right)^2 + \left(\frac{\delta T_3}{T_3}\right)^2 + \left(\frac{\delta R_{solder}}{R_{solder}}\right)^2 + \left(\frac{\delta k_{CS}}{k_{CS}}\right)^2 + \left(\frac{\delta x_{CS}}{x_{CS}}\right)^2} \tag{8}$$

A summary of the uncertainties was listed in Table 1.

3. Results and discussion

3.1. Boiling curves

The detailed working conditions are shown in Table 2. To ensure the repeatability, every experimental condition was carried out twice and denoted as 1 and 2 as shown in Fig. 4.

From boiling curves, there is a slight deviation in the superheating between two experiments. The reasons can be summarized as follows.

(1) The surface was polished by hands. No certain patterns of local surface structure could be obtained, which might cause different local temperature profiles.
(2) Local parts of the surface might be oxidized during experiment. However, oxidation was random without certain modes. So, some differences in superheating were likely to occur in different experiment.

However, the CHF was similar for two experiments, which was the main interest of the experiment.

To validate CHF values, an empirical correlation was chosen. Katto and Kurata [27] conducted an upward flow boiling experiment using copper to investigate effects of mass flux and heater length, and concluded the CHF correlation as follows

$$q_{CHF} = 0.186 G h_{fg} \left(\frac{\rho_g}{\rho_f}\right)^{0.559} \left(\frac{\sigma \rho_f}{G^2 L}\right)^{0.264} \tag{9}$$

where G stands for the mass flux of the liquid, and L is the length of the heated surface.

In Fig. 5, aluminum shows the biggest CHF, while carbon steel CHF is lower. CHFs of copper is close to Eq. (9). Even though the

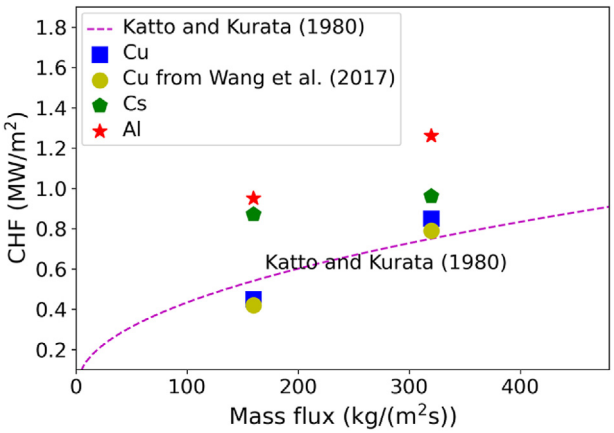

Fig. 5. CHF change with mass flux for different materials.

same sandpaper was applied to each surface, it showed different CHF results. A previous experiment result from Wang et al. [28] was also adopted to confirm the repeatability. The different CHFs for materials have been demonstrated in previous pool boiling experiments. For example, Mei et al. [16] conducted a pool boiling experiment and found that compared to copper and stainless steel, carbon steel had a higher CHF. Kim et al. [10] conducted experiments in a pool boiling experiment and found that aluminum had a higher CHF than copper. However, the research of material effects was mainly studied in the pool boiling field. The experiments on flow boiling were quite few. Still, the mechanism behind this need to be explained.

3.2. Discussion

In the present study, the heater length is 30 mm the bubble generation and sliding can be captured easily for this length. However, it was well-known that heater length had some effects on nucleate boiling. For example, Kam et al. [29] investigated the different heater width from 40 mm to 60 mm. Ahn et al. [30] investigated the ziracloy surface using a test piece of 20 mm * 25 mm. Gaertner [31] conducted a photographic study on pool boiling using a spherical shape with a diameter of 50.8 mm. In this study, experiments were conducted on the same size blocks. However, the scale effect was not within the scope of our manuscript. It may need further investigations.

Table 3
Physical properties of copper, carbon steel, and aluminum (around 300 K).

Material	ρ (kg m^{-3})	c_p (Jkg^{-1} K^{-1})	k (Wm^{-1} K^{-1})	$\sqrt{\rho c_p k}$
Copper	8960	385	401	37193
Carbon steel	7850	460	50	13437
Aluminum	2700	897	237	23958

There are different opinions on the reason of the CHF difference. They are mainly related to one or combined effects of the following factors: contact angle, surface roughness, thermal effusivity and nucleation sites.

After experiments, all surfaces showed different degree of oxidation. Due to the randomness of oxidation process, the surface after oxidation exhibited uneven black dots, which was most obvious in carbon steel case as shown in Fig. 6. A similar case for carbon steel is in Lee et al. [18]. They performed pool boiling experiments using SA508 and found that CHF gradually increased with surface change due to corrosion. The corrosion product was analyzed to be magnetite generated by oxidation. Mei et al. [16] found the surface corrosion and attributed it to the increase of wettability and porous structure. In Vlachou et al. [32], copper was found to have different superheating under different boiling time condition. Lee and Chang [18] put a test ribbon made of SA508 into water for different time. CHF was found to have increased after immersion in water for 50 min the surface color turned black with boiling time. The Scanning Electron Microscopy (SEM) and Energy Dispersive X-Ray Analysis (EDX) showed that surface roughed and corrosion particles existed on the heating surface.

It was reported that surface morphology had a great influence on the heat transfer. The contact angle and surface roughness were measured before and after each experiment. To measure the contact angle, a droplet was dropped on to the heating surface. And then images were processed to measure the contact angle using ImageJ. At least six contact angle values were obtained. The average of the six values was taken as the contact angle and standard deviation was adopted as the measurement uncertainty. All contact angles after experiments showed different levels of decrease. This is thought to be related to oxidation effects. The oxidation layer formed on the surface created a porous layer which allowed water to spread on the surface. In Lee et al. [5], after oxidation, zircaloy surface showed some decrease of contact and an enhancement of

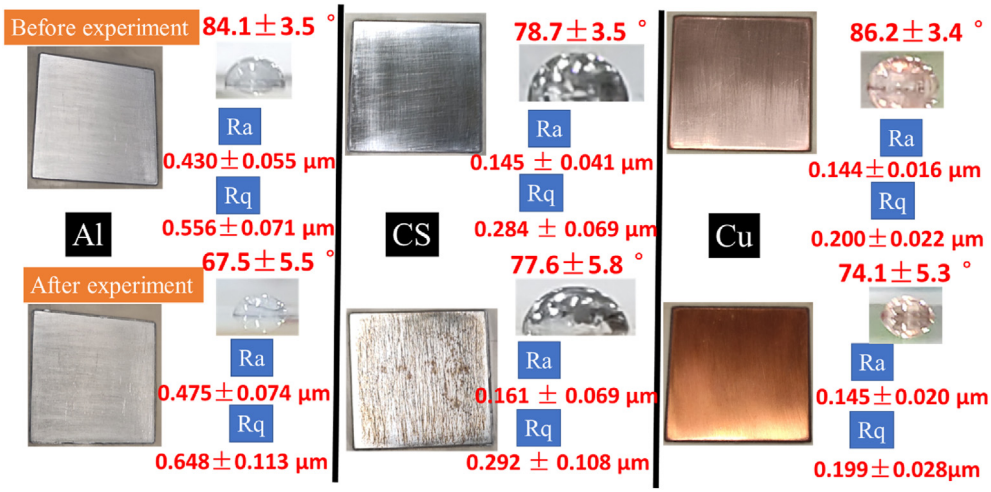

Fig. 6. Surface properties for the three materials before and after experiment.

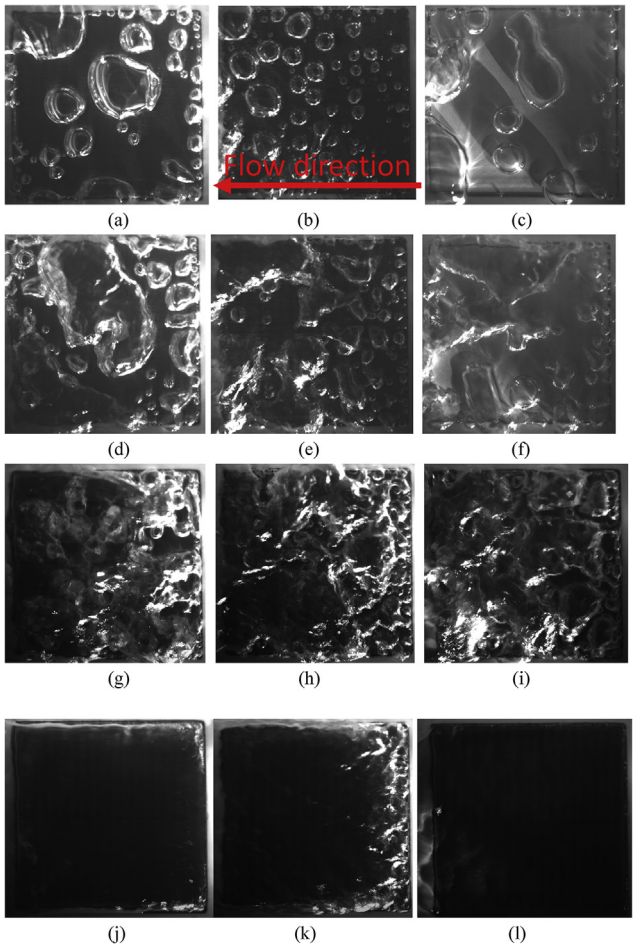

Fig. 7. Images of the surfaces during experiments under different heat flux, mass flux = 160 kg/(m^2 s). Experiments of (a) copper, (b) carbon steel, (c) aluminum, with a heat flux of around 0.09 MW/m^2. Experiments of (d) copper, (e) carbon steel, (f) aluminum, with a heat flux of around 0.18 MW/m^2. Experiments of (g) copper, (h) carbon steel, (i) aluminum, with a heat flux of around 0.46 MW/m^2. Experiments of (j) copper, (k) carbon steel, (l) aluminum around CHF point.

CHF. In Son et al. [33], when carbon steel was oxidized for up to 40 days, a decrease of contact angle was found. Wang et al. [34] conducted flow boiling experiments to study the oxidation effect on copper. An increase of CHF and wettability was found after the surface was oxidized. Ahn et al. [30] anodized a zircaloy-4 surface in a pool boiling experiment. It was found that surface had a big increase of wettability with an increase in CHF.

To measure the surface roughness, a portable surface roughness meter SJ210 (Mitutoyo) was used. The meter has a probe tip radius of 2 μm with a measuring force of 0.75 mN. Due to the non-uniform surface roughness, we measured several different locations. Usually, at least six different locations were measured. Aluminum is softer with a Mohs hardness of 2.5–3, and copper is harder with a Mohs hardness of 3. Carbon steel is hardest with a Mohs hardness of 4–4.5 [35]. Therefore, aluminum surface had the largest roughness. Carbon steel and copper had similar roughness which was probably because the sandpaper used in the experiment had reached to its maximum ability of surface smoothing. After experiment, surface roughness of both aluminum and carbon steel increased due to the corrosion of the surface, while copper surface showed very slight change after experiments. However, the uncertainties of surface roughness became bigger showing the uniform oxidation degree on different regions. Oxidized particles generated during nucleate boiling filled the pores, scratches of the heating surface, making the surface rougher after experiment. Ji et al. [36] conducted pool boiling experiments under nanofluid water, an increase of surface roughness after experiment was also found and attributed to the deposition of nanoparticles. Kim et al. [37] examined the Cr-coated surface and found more oxygen elements formed on the post-CHF surface than the initial surface. They explained that it was because the sudden surge of temperature led to the rapid surface oxidation. The sudden temperature surge was caused by vapor covering the heating surface at CHF point. Interestingly, in Kim et al. [38], both experiments on copper and aluminum were conducted. It was found that after polishing by the same type of sandpapers, aluminum showed higher CHF than copper for pool boiling experiments, which agreed with our experimental results. However, even at the same initial surface roughness, aluminum CHF was higher than that copper CHF. This demonstrated that roughness alone was not able to explain the difference of CHFs.

Another important factor was thermal effusivity. Table 3 shows the physical properties of the three materials. Copper has the higher thermal effeusivity than that of carbon steel and aluminum. Usually, higher thermal effeusivity indicates a higher CHF. For example, Mei et al. [16] found that stainless steel has a lower CHF than copper, which was explained by the smaller thermal effeusivity of stainless steel. Kam et al. [28] conducted pool boiling experiments to investigate material effects. They pointed out that contact angle alone could not explain the CHF difference. other factors like thermal effusivity should be taken into consideration. However, copper has the lowest CHF in this study. This is related to the easiness of oxidation of aluminum and carbon steel surface. The oxidation of carbon steel was obvious from the surface corrosion. Kim et al. [38] pointed that unlike copper or stainless steel, aluminum could react with hot water above 80 °C, which easily enhanced wettability. Min and Webb [39] found that aluminum oxide hydroxide could be formed on the aluminum surface when dipping into hot water.

Fig. 7 and Fig. 8 show surface images during experiments under different heat flux, mass flux = 160 kg/(m^2 s) and 320 kg/(m^2 s), respectively. For 160 kg/(m^2 s) case, under low heat flux, carbon steel surface generated more bubbles than copper and aluminum surface, which correspond to the low superheating of carbon steel. For 320 kg/(m^2 s) case, under low heat flux, the surface of the three materials generated fewer bubbles than mass flux = 320 kg/(m^2 s). Furthermore, the number of bubbles on three materials was similar, which agreed with similar superheating of the three materials for 320 kg/(m^2 s) case. Under high heat flux, bubbles of copper tended to coalesce with each other, covered the heating surface preventing water from supplying into the surface. For aluminum, bubbles were more separated and scattered on the heating surface, allowing more water to supply into the surface, which might lead to bigger CHF. When CHF occurred, a continuous vapor film formed above the heater surface, which caused the boiling crisis.

4. Conclusions

To study material effects of CHF, downward-facing experiments were conducted at atmospheric pressure. Aluminum, copper, and carbon steel were used. The main conclusions are:

(1) Different materials have different CHFs. Aluminum has the biggest CHF while copper has the smallest CHF for each mass flux.
(2) After experiment, surface wettability increased and surface became rougher, which was due to the oxidation process during nucleate boiling.

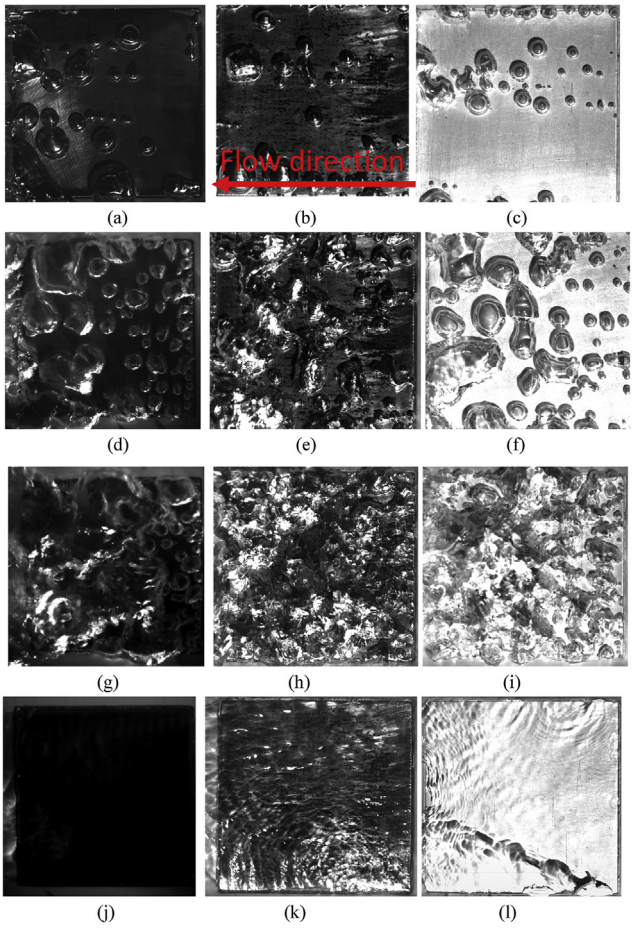

Fig. 8. Images of the surfaces during experiments under different heat flux, mass flux = 320 kg/(m^2 s). Experiments of (a) copper, (b) carbon steel, (c) aluminum, with a heat flux of around 0.09 MW/m^2. Experiments of (d) copper, (e) carbon steel, (f) aluminum, with a heat flux of around 0.18 MW/m^2. Experiments of (g) copper, (h) carbon steel, (i) aluminum, with a heat flux of around 0.46 MW/m^2. Experiments of (j) copper, (k) carbon steel, (l) aluminum around CHF point.

(3) The CHF difference of different materials is related to the surface wettability, roughness, thermal effusivity, and nucleation sites.

We have confirmed that for the downward-facing condition, different materials have different CHFs. Even though the same type of sandpaper was used, aluminum has the highest CHF while copper has the lowest. It was found that different materials had different surface wettability, roughness, thermal effusivity and number of bubbles. However, it was difficult to tell which factor was dominant. Further studies are needed to investigate the mechanism.

Declaration of competing interest

We declare that we have no conflict of interest.

Acknowledgments

This work was supported by the Japan Grant-in-Aid for Scientific Research (B) (Grand No. 19H02645) and the Ministry of Education, Culture, Sports, Science and Technology of Japan (MEXT) (Grand No. 1081782).

References

[1] C.M. Patil, S.G. Kandlikar, Pool boiling enhancement through microporous coatings selectively electrodeposited on fin tops of open microchannels, Int. J. Heat Mass Tran. 79 (2014) 816–828.
[2] T. Wu, P.S. Lee, J. Mathew, S.R. Lu, Experimental study of ageing effect in pool boiling heat transfer. 20th electronics packaging Technology conference (EPTC), IEEE (2018) 477–484.
[3] N.I. Kolev, How accurately can we predict nucleate boiling? Exp. Therm. Fluid Sci. 10 (3) (1995) 370–378.
[4] B.R. Sehgal, Nuclear Safety in Light Water Reactors: Severe Accident Phenomenology, second ed., Elsevier, San Diego, 2012.
[5] C.Y. Lee, T.H. Chun, W. Kee In, Critical heat flux of oxidized zircaloy surface in saturated water pool boiling, J. Nucl. Sci. Technol. 52 (4) (2015) 596–606.
[6] S.G. Kandlikar, A theoretical model to predict pool boiling CHF incorporating effects of contact angle and orientation, J. Heat Tran. 123 (2001) 1071–1079.
[7] K. Wang, N. Erkan, H. Gong, K. Okamoto, Effects of carbon steel surface oxidation on critical heat flux in downward-face pool boiling, Int. J. Heat Mass Tran. 136 (2019) 470–485.
[8] K. Wang, N. Erkan, K. Okamoto, A study on the effect of oxidation on critical heat flux in flow boiling with downward-faced carbon steel, Int. J. Heat Mass Tran. 147 (2020) 118966.
[9] H. O'Hanley, C. Coyle, J. Buongiorno, T. McKrell, L.-W. Hu, M. Rubner, R. Cohen, Separate effects of surface roughness, wettability, and porosity on the boiling critical heat flux, Appl. Phys. Lett. 103 (2013), 024102.
[10] J. Kim, S. Jun, R. Laksnarain, S.M. You, Effect of surface roughness on pool boiling heat transfer at a heated surface having moderate wettability, Int. J. Heat Mass Tran. 101 (2016) 992–1002.
[11] R. Braun, Wärmeübergang beim Blasensieden an der Außenseite von geschmirgelten und sandgestrahlten Rohren aus Kupfer, Messing und Edelstahl, Doctor dissertation, University Fridericiana Karlsruhe, 1992.
[12] X. Zhou, K. Bier, Influence of the heat conduction properties of the wall material and of the wall thickness on pool boiling heat transfer, in: EUROTHERM Seminar No. 48: Pool Boiling 2, Paderborn, Germany, 1996.
[13] U. Magrini, E. Nannei, On the influence of the thickness and thermal properties of heating walls on the heat transfer coefficients in nucleate pool boiling, J. Trans ASME Heat Transfer (1975) 173–178.
[14] V.A. Grigoriev, V.V. Klimenko, Y.M. Pavlov, E.V. Ametistov, Influence of Some Heating Surface Properties on the Critical Heat Flux in Cryogenic Liquids Boiling, Begel House Inc, 1978.
[15] J.W. Westwater, J.J. Hwalek, M.E. Irving, Suggested standard method for obtaining boiling curves by quenching, Ind. Eng. Chem. Fundam. 25 (4) (1986) 685–692.
[16] Y. Mei, Y. Shao, S. Gong, Y. Zhu, H. Gu, Effects of surface orientation and heater material on heat transfer coefficient and critical heat flux of nucleate boiling, Int. J. Heat Mass Tran. 121 (2018) 632–640.
[17] C. Bombardieri, C. Manfletti, Influence of wall material on nucleate pool boiling of liquid nitrogen, Int. J. Heat Mass Tran. 94 (2016) 1–8.
[18] J. Lee, S.H. Chang, An experimental study on CHF in pool boiling system with SA508 test heater under atmospheric pressure, Nucl. Eng. Des. 250 (2012) 720–724.
[19] H.M. Park, Y.H. Jeong, S. Heo, Effect of heater material and coolant additives on CHF for a downward facing curved surface, Nucl. Eng. Des. 278 (2014) 344–351.
[20] D.H. Kam, Y.J. Choi, Y.H. Jeong, CHF experiment with downward-facing carbon and stainless steel plates under pressurized conditions, Int. J. Heat Mass Tran. 125 (2018) 670–680.
[21] D.H. Kam, Y.J. Choi, Y.H. Jeong, H.C. No, Heat transfer performance of downward-facing carbon and stainless steel surfaces, Int. Commun. Heat Mass Tran. 113 (2020) 104503.
[22] L. Liao, R. Bao, Z. Liu, Compositive effects of orientation and contact angle on critical heat flux in pool boiling of water, Heat Mass Tran. 44 (2008) 1447–1453.
[23] M.S. El-Genk, A.F. Ali, Enhanced nucleate boiling on copper micro-porous surfaces, Int. J. Multiphas. Flow 36 (2010) 780–792.
[24] K. Wang, H. Gong, L. Wang, N. Erkan, K. Okamoto, Effects of a porous honeycomb structure on critical heat flux in downward-facing saturated pool boiling, Appl. Therm. Eng. 166 (2020) 115036.
[25] I. Golobič, A.E. Bergles, Effects of heater-side factors on the saturated pool boiling critical heat flux, Exp. Therm. Fluid Sci. 15 (1) (1997) 43–51.
[26] R.J. Moffat, Describing the uncertainties in experimental results, Exp. Therm. Fluid Sci. 1 (1) (1988) 3–17.
[27] Y. Katto, C. Kurata, Critical heat flux of saturated convective boiling on uniformly heated plates in a parallel flow, Int. J. Multiphas. Flow 6 (6) (1980) 575–582.
[28] L. Wang, A.R. Khan, N. Erkan, H. Gong, K. Okamoto, Critical heat flux enhancement on a downward face using porous honeycomb plate in saturated flow boiling, Int. J. Heat Mass Tran. 109 (2017) 454–461.
[29] D.H. Kam, Y.J. Choi, Y.H. Jeong, Critical heat flux on downward-facing carbon steel flat plates under atmospheric condition, Exp. Therm. Fluid Sci. 90 (2018) 22–27.
[30] H.S. Ahn, C. Lee, H. Kim, et al., Pool boiling CHF enhancement by micro/nanoscale modification of zircaloy-4 surface, Nucl. Eng. Des. 240 (10) (2010) 3350–3360.

[31] R.F. Gaertner, Photographic study of nucleate pool boiling on a horizontal surface, J. Heat Tran. 87 (1965) 17–27.
[32] M.C. Vlachou, J.S. Lioumbas, K. David, D. Chasapis, T.D. Karapantsios, Effect of channel height and mass flux on highly subcooled horizontal flow boiling, Exp. Therm. Fluid Sci. 83 (2017) 157–168.
[33] H.H. Son, U. Jeong, G.H. Seo, S.J. Kim, Oxidation effect on the pool boiling critical heat flux of the carbon steel substrates, Int. J. Heat Mass Tran. 93 (2016) 1008–1019.
[34] K. Wang, N. Erkan, K. Okamoto, Oxidation effect of copper on the downward-facing flow boiling CHF under atmospheric condition, Int. J. Heat Mass Tran. 156 (2020) 119866.
[35] https://en.wikipedia.org/wiki/Mohs_scale_of_mineral_hardness.
[36] W.T. Ji, P.F. Zhao, C.Y. Zhao, J. Ding, W.Q. Tao, Pool boiling heat transfer of water and nanofluid outside the surface with higher roughness and different wettability, Nanoscale Microscale Thermophys. Eng. (2018) 296–323.
[37] N. Kim, H.H. Son, S.J. Kim, Oxidation effect on pool boiling critical heat flux enhancement of Cr-coated surface for accident-tolerant fuel cladding application, Int. J. Heat Mass Tran. 144 (2019) 118655.
[38] J. Kim, S. Jun, J. Lee, S.M. You, Effect of surface roughness on pool boiling heat transfer of water on a superhydrophilic aluminum surface, J. Heat Transfer 139 (1) (2017) 101501.
[39] J. Min, Webb, Long-Term Wetting and Corrosion Characteristics of Hot Water Treated Aluminum and Copper Fin Stocks, Int. J. Refrig 25 (8) (2002) 1054–1061.